HHS Public Access

Author manuscript

Psychophysiology. Author manuscript; available in PMC 2017 November 01.

Published in final edited form as:

Psychophysiology. 2016 November ; 53(11): 1627–1638. doi:10.1111/psyp.12731.

Large-scale Functional Brain Connectivity during Emotional Engagement as Revealed by Beta-series Correlation Analysis

Daesung Kang[1], **Yuelu Liu**[1], **Vladimir Miskovic**[2], **Andreas Keil**[3], and **Mingzhou Ding**[1]

[1]The J. Crayton Pruitt Family Department of Biomedical Engineering, University of Florida, Gainesville, Florida 32611

[2]Department of Psychology and Center for Affective Science, State University of New York at Binghamton, Binghamton, NY 13901

[3]Department of Psychology and Center for the Study of Emotion and Attention, University of Florida, Gainesville, Florida 32611

Abstract

It has been hypothesized that the medial prefrontal cortex (mPFC) is a hub in the network that mediates appetitive responses whereas the amygdala is thought to mediate both aversive and appetitive processing. Both structures may facilitate adaptive responses to emotional challenge by linking perception, attention, memory, and motor circuits. We provide an initial exploration of these hypotheses by recording simultaneous EEG-fMRI in eleven participants viewing affective pictures. MPFC- and amygdala-seeded functional connectivity maps were generated by applying the beta-series correlation method. The mPFC-seeded correlation map encompassed visual regions, sensorimotor areas, prefrontal cortex, and medial temporal lobe structures, exclusively for pleasant content. For the amygdala-seeded correlation map, a similar set of distributed brain areas appeared in the unpleasant-neutral contrast, with the addition of such subcortical structures as insula and thalamus. A substantially sparser network was recruited for the pleasant-neutral contrast. Using the late positive potential (LPP) to index the intensity of emotional engagement, functional connectivity was found to be stronger in trials with larger LPP. These results demonstrate that mPFC-mediated functional interactions are engaged specifically during appetitive processing, whereas the amygdala is coupled to distinct sets of brain regions during both aversive and appetitive processing. The strength of these interactions varies as a function of the intensity of emotional engagement.

Emotions are rooted in ancient cortico-limbic survival circuits that generate behavioral dispositions in response to appetitive and aversive exteroceptive signals (Lang & Bradley, 2010; LeDoux, 2012). In humans, exposure to affectively arousing stimuli triggers activity in multiple brain regions that coalesce into large-scale functional assemblies (Lindquist, Wager, Kober, Bliss-Moreau, & Barrett, 2012; Pessoa & Adolphs, 2010). The amygdala and mPFC are thought to form communication hubs within these assemblies (Kinnison, Padmala, Choi, & Pessoa, 2012), owing to their dense interconnectivity with many regions of the brain supporting perceptual-motor processing and behavioral control (Swanson, 2000; Young,

Correspondence: Mingzhou Ding (mding@bme.ufl.edu) and Andreas Keil (akeil@ufl.edu).

Scannell, Burns, & Blakemore, 1994). Accordingly, understanding their functional interaction with other brain regions during emotional engagement is not only a major goal of systems neuroscience but it may also hold important clues for revealing impaired network activity in various affective disorders (Lang & Bradley, 2010).

Many brain regions related to affective processing exhibit increased hemodynamic activity during both aversive and appetitive challenge (Bradley, et al., 2015; Lindquist, Wager, Kober, Bliss-Moreau, & Barrett, 2012; Sabatinelli, Keil, Frank, & Lang, 2013). Abundant evidence, however, also exists for valence-specific affective networks within the human brain. Studies have reported findings consistent with the existence of a core aversive/defensive network that responds either specifically to socially aversive inputs (Seymour, Singer, & Dolan, 2007) or to aversive information in general (Hayes & Northoff, 2011). The amygdala and the anterior insula are often mentioned as crucial components of this core aversive network (Fan, et al., 2011). On the other hand, studies using high-arousing appetitive and aversive stimuli have reliably observed amygdala engagement for emotionally arousing stimuli, irrespective of hedonic valence (Lang & Bradley, 2010). For example, connectivity between the left amygdala and perihippocampal regions measured by hemodynamic imaging predicted report accuracy in a memory task with emotional pictures (Ritchey, Dolcos, & Cabeza, 2008). In general, viewing emotionally salient stimuli has been associated with heightened activity in the so-called salience network (Seeley et al., 2007) encompassing structures such as the dorsal anterior cingulate cortex (ACC), ventrolateral prefrontal cortex, and anterior insula, in addition to the amygdala (Touroutoglou, Bickart, Barrett, & Dickerson, 2014). While the amygdala is clearly responsive to emotional arousal (intensity) in general, an untested hypothesis is whether the specific signature of distributed network interactions between the amygdala and other structures exhibits motive system (i.e., appetitive versus defensive) specificity (Pessoa, 2014). The first goal of the present study is to address this hypothesis.

For appetitive processing, converging evidence suggests a central role for the nucleus accumbens (NAcc) and mPFC. Enhanced hemodynamic responses in NAcc/mPFC have been observed to be specific to the viewing of appetitive stimuli (Sabatinelli, Bradley, Lang, Costa, & Versace, 2007). Interestingly, mPFC activity dropped below baseline when viewing images with neutral or aversive content (Sabatinelli, Flaisch, Bradley, Fitzsimmons, & Lang, 2004). Extending this research, imagining pleasant scenes also led to NAcc and mPFC recruitment, and the functional connectivity between these regions and the amygdala uniquely characterized the imagery of pleasant affective content (Costa, Lang, Sabatinelli, Versace, & Bradley, 2010). The mPFC tends to be reliably engaged during appetitive engagement in a variety of emotion-induction paradigms, including picture viewing, reading, and mental imagery (see e.g., Costa, Lang, Sabatinelli, Versace, & Bradley, 2010). Based on these findings and our preliminary data we hypothesize that mPFC functionally interacts with other brain structures, including areas in the perceptual-motor system, during appetitive processing specifically. The second goal of this study is to examine this hypothesis.

Another important factor that influences large-scale brain network responses concerns the intensity of emotional engagement. As with many other complex brain functions, emotional processing exhibits substantial trial-by-trial variability depending on the eliciting stimuli and

the functional state of the brain. Numerous studies indicate that the late positive potential (LPP) reliably indexes the degree of emotional arousal and processing intensity (Cuthbert, Schupp, Bradley, Birbaumer, & Lang, 2000; Keil, et al., 2002; Schupp, et al., 2004). The LPP has been shown to be associated with BOLD responses in distributed brain areas (Liu, Huang, McGinnis-Deweese, Keil, & Ding, 2012; Sabatinelli, Keil, Frank, & Lang, 2013; Sabatinelli, Lang, Keil, & Bradley, 2007). It is thus reasonable to expect that the strength of functional interactions between hub regions such as the amygdala and mPFC and other brain areas should be modulated by the relative intensity of emotional processing. The third goal of our study is to test this hypothesis by applying a multimodal neuroimaging approach.

These three goals were achieved by re-analyzing data from a previous study (Liu, Huang, McGinnis-Deweese, Keil, & Ding, 2012) in which we recorded simultaneous fMRI and EEG during free viewing of affective pictures containing pleasant, unpleasant, and neutral scenes. For hemodynamic data, amygdala- and mPFC-seeded functional connectivity were assessed using the beta-series correlation method (Rissman, Gazzaley, & D'Esposito, 2004), which has previously been employed in studies of emotional processing (Iordan & Dolcos, 2015). LPP amplitude was estimated from the EEG data to provide an objective, electrophysiological index of emotional engagement for each individual and each image presentation. The LPP has previously been identified as having desirable psychometric properties (Moran, Jendrusina, & Moser, 2013), and can be estimated from single trials (Liu, Huang, McGinnis-Deweese, Keil, & Ding, 2012). Our analysis was focused on aversive versus neutral and appetitive versus neutral contrasts. Within each contrast, functional connectivity was further parsed by separating low and high LPP amplitude trials.

Method

Participants

Fifteen healthy volunteers with normal or corrected-to-normal vision participated in the experiment in exchange for either course credits or a financial incentive of $30. The experimental protocol was approved by the Institutional Review Board of the University of Florida. Written informed consent was obtained from all participants before the experiment. One participant withdrew from the experiment. In addition, data from three participants were discarded due to excessive EEG artifacts. The remaining 11 participants (7 females; mean age, 20 yrs.; SD, 2.65) performed the task according to instructions, provided data at a quality that allowed for single-trial EEG analysis (see methods), and thus were included in the analysis.

Stimuli

The stimuli consisted of 20 pleasant, 20 neutral, and 20 unpleasant pictures selected from the International Affective Picture System (IAPS) based on their content, as well as their normative hedonic valence and emotional arousal ratings (Lang, Bradley, & Cuthbert, 2008). The IAPS picture numbers of these stimuli were: Pleasant: 4311, 4599, 4610, 4624, 4626, 4641, 4658, 4680, 4694, 4695, 2057, 2332, 2345, 8186, 8250, 2655, 4597, 4668, 4693, 8030. Neutral: 2398, 2032, 2036, 2037, 2102, 2191, 2305, 2374, 2377, 2411, 2499, 2635, 2347, 5600, 5700, 5781, 5814, 5900, 8034, 2387. Unpleasant: 1114, 1120, 1205, 1220,

1271, 1300, 1302, 1931, 3030, 3051, 3150, 6230, 6550, 9008, 9181, 9253, 9420, 9571, 3000, 3069. The pictures were selected to cover a wide range of contents to avoid category-specific brain activity, such as that evoked by only erotic scenes, and to enable robust appetitive and aversive engagements across observers. The pleasant pictures included sport scenes, romance, and erotic couples, whereas the unpleasant pictures included threat, attack scenes, and bodily mutilations. The neutral pictures included landscapes and neutral human beings. Across contents, pictures were matched for presence/absence of living/non-living content, as well as for landscape/scene versus close-up shots, and they were also matched for in-house ratings of perceived complexity obtained from several hundreds of undergraduate students in a preliminary rating study.

The mean pleasure (valence) rating for pleasant, neutral, and unpleasant pictures was 7.0, 6.3, and 2.8, respectively. The pleasant and unpleasant pictures had similar mean arousal levels (pleasant, 5.8; unpleasant, 5.9), both being higher than neutral pictures (4.2). Statistical tests of these means showed that the three picture categories differed in reports of hedonic valence, as expected (pleasant > neutral, $t(38)=2.7$, $p=.01$; pleasant > unpleasant, $t(38)=18.7$, $p<0.001$; neutral > unpleasant, $t(38)=9.9$, $p<0.001$). Also as expected, rated emotional arousal did not differ between pleasant and unpleasant pictures, $t(38)=1.1$, $p=0.27$, but did differ between pleasant and neutral, $t(38)=6.1$, $p<0.001$; and unpleasant and neutral pictures, $t(38)=7.0$, $p<0.001$. Despite these differences, it should be noted that the three categories did not show strong mean differences in affective ratings. Specifically, neutral pictures were high in rated pleasantness potentially representing a threat to the validity of neutral-pleasant comparisons. The selection of pictures was guided by two considerations: (1) that affective ratings capture one important aspect of the emotional reactivity related to viewing IAPS, but other dimensions such as physiological reactivity tend to capture other, also important, aspects of emotional reactivity, sometimes to be balanced against the facets of emotion captured by ratings, and (2) that the overall position of a given picture in the affective space on both dimensions (hedonic valence and emotional arousal) rather than on each dimension was particularly important to us for this study, in which a wide range of contents was targeted rather than relying on narrow content categories. In previous work with this stimulus set, we observed robust separation between categories while maintaining high experimental control (Miskovic et al., 2015), leading us to seek this compromise between clear separation of emotion categories in terms of ratings versus in terms of physiological measures such as the LPP. Hence, replication with a set of pictures showing greater spread between categories in terms of hedonic valence and emotional arousal is desirable.

Procedure

The experiment was implemented in an event-related fMRI design using E-Prime software. Each IAPS picture was centrally displayed on an MR-compatible monitor for 3 seconds followed by a variable (2800 or 4300 ms) interstimulus interval. Participants viewed the images in the scanner via a reflective mirror system. There were five viewing blocks of 60 trials each. A break was given between blocks. In each block, the same 60 pictures were repeated in different random orders. The order of picture presentation was further randomized across different participants. A fixation cross was displayed at the center of the

screen. Before the start of the experiment, participants were instructed to fixate on the central cross and to view the pictures without moving their eyes. After the experiment participants were invited to rate 12 representative pictures (4 pictures within each category) they had not seen during the experiment on scales of hedonic valence and emotional arousal, using a paper and pencil version of the self-assessment manikin (Bradley & Lang, 1994). The purpose of these ratings was to quantify the extent to which the picture categories used here induced affective responses in the observers (see e.g., Codispoti, Ferrari, & Bradley, 2006).

We note that previous neuroimaging work examining effects of emotional scene repetition has demonstrated that repetition effects and emotion effects do not interact in terms of BOLD (Bradley et al., 2015). Similarly, the LPP emotion effect has been robustly established as being unaffected by intermittent (i.e. non-massed) repetition (Bradley, 2009; Codispoti, Ferrari, & Bradley, 2006; Ferrari, Bradley, Codispoti, & Lang, 2011). In combination with explicit control for any repetition effects (see below), these considerations allowed us to treat the five blocks of trials equally, generating greater power and signal-to-noise ratios. Because the entire experiment lasted approximately 40 minutes, this being in addition to the extensive EEG preparation time, a decision was made not to invite affective ratings during the experiment on a trial-by-trial basis. Doing so would have lengthened the session dramatically, reduced signal quality, and possibly induced more motion artifacts.

Data acquisition

MRI data were collected on a 3T Philips Achieva scanner (Philips Medical Systems). Two hundred and twelve volumes of functional images were acquired using a gradient-echo echoplanar imaging (EPI) sequence during each session [echo time (TE), 30 ms; repetition time (TR), 1.98 s; flip angle, 80°; slice number, 36; field of view, 224 mm; voxel size, 3.5×3.5×3.5 mm; matrix size, 64×64]. The slices were acquired in ascending order and oriented parallel to the plane connecting the anterior and posterior commissure.

EEG data were recorded using a 32-channel MR-compatible EEG system (Brain Products GmbH). Thirty-one sintered Ag/AgCl electrodes were placed on the scalp according to the 10-20 system, and one additional electrode was placed on subject's upper back to monitor electrocardiograms (ECG). The recorded ECG was used to detect heartbeat events that subsequently aided in the removal of the cardioballistic artifacts. The EEG channels were referenced to the FCz electrode during recording. EEG signal was recorded with an online 0.1~250 Hz band-pass filter and digitized to 16 bit at a sampling rate of 5 kHz. The EEG recording system was synchronized with the scanner's internal clock throughout the recording session to ensure the successful removal of the gradient artifact in subsequent analyses.

Data preprocessing

The fMRI data were preprocessed using SPM5 (http://www.fil.ion.ucl.ac.uk/spm/). The first five volumes in each experimental session were discarded to eliminate transient effects. Slice timing was corrected using interpolation to account for differences in slice acquisition time. The images were then corrected for head movement by spatially realigning them to the sixth

image of each session, normalized and registered to the Montreal Neurological Institute (MNI) template, and resampled to a spatial resolution of 3 × 3 × 3 mm. The transformed images were smoothed by a Gaussian filter with a full-width at half-maximum of 8 mm. The low-frequency temporal drifts were removed from the functional images by applying a high-pass filter with a cutoff frequency of 1/128 Hz, and the global signal was removed by dividing every voxel in a slice by the estimated global signal value.

Brain Vision Analyzer 2.0 (Brain Products GmbH) was used to remove scanner artifacts in the EEG data. The gradient artifacts were removed by using a modified version of the original algorithms proposed by Allen et al. (Allen, Josephs, & Turner, 2000). Briefly, an artifact template was created by segmenting and averaging the data according to the onset of each volume within a sliding window consisting of 41 consecutive volumes, and subtracted from the raw EEG data. The cardioballistic artifacts were removed by using an average artifact subtraction method (Allen, Polizzi, Krakow, Fish, & Lemieux, 1998). In this method R peaks were detected in the low-pass-filtered ECG signal and used to construct a delayed average artifact template over 21 consecutive heartbeat events. The average artifact template was subtracted from the original EEG signal in a sliding-window approach. The EEG data after these two steps were low-pass filtered with the cutoff set at 50 Hz, down-sampled to 250 Hz, and re-referenced to the average reference. These data were then exported to EEGLAB (Delorme & Makeig, 2004) and SOBI (Second Order Blind Identification; Belouchrani, Abed-Meraim, Cardoso, & Moulines, 1993) was applied to further correct for eye-blinking, residual cardioballistic, and movement-related artifacts. The artifact-corrected data were then epoched from −300 ms to 2000 ms with 0 ms representing image onset. The pre-stimulus baseline was defined as −300 to 0 ms for ERP analysis (Liu, Huang, McGinnis-Deweese, Keil, & Ding, 2012).

Seed region selection

Our previous work on the same data has reported fMRI activation by contrasting pleasant versus neutral pictures and unpleasant versus neutral pictures employing the general linear model (GLM) approach (Liu, Huang, McGinnis-Deweese, Keil, & Ding, 2012). The published activation maps became the basis for selecting mPFC and amygdala seed regions in the present study. For mPFC, a sphere of 5-mm in radius centered at the most activated voxel in mPFC (MNI coordinate [9, 60, 3]) under the group-level contrast of pleasant versus neutral was selected as the seed region. For amygdala, the spheres for the left and right amygdala were similarly chosen under the group-level contrast of unpleasant versus neutral (center coordinates for left and right amygdala: [−21, 0, −18] and [21, 0, −18]). Because left and right amygdala yielded similar connectivity patterns they were combined into a single amygdala seed. As discussed in the Introduction, the choice of mPFC and amygdala as seed regions was well grounded in previous studies, reflecting their distinct involvement in the processing of appetitive and aversive pictures (Sabatinelli, et al., 2011; Sabatinelli, Lang, Keil, & Bradley, 2007). Seed regions were also based on findings with an earlier analysis of this data (Liu et al., 2012), in which mPFC and amygdaloid BOLD activation were found to co-vary with the LPP in a content-specific fashion.

Functional connectivity

We applied the beta-series correlation method to assess functional interactions between the seed region and other brain regions (Rissman, Gazzaley, & D'Esposito, 2004; Rissman, Gazzaley, & D'Esposito, 2008). In this method, beta values representing the extent of brain activation were estimated for each single trial using the GLM approach. For each participant 300 covariates of interest (5 sessions with 60 picture trials each) were introduced into the GLM design matrix to model the hemodynamic response elicited by each picture presentation (Axmacher, Schmitz, Wagner, Elger, & Fell, 2008; Chadick & Gazzaley, 2011; Rissman, Gazzaley, & D'Esposito, 2004). Nuisance factors such as head movements were included in the model as additional regressors of no interest. For a given group of trials, the beta-series from the seed region was correlated with the time series from every other voxel in the brain using Pearson's correlation, with higher correlation coefficients assumed to indicate stronger inter-area functional connectivity. The correlation coefficients were standardized into z-scores using Fisher's r-to-Z transform for further statistical analysis (Rissman, Gazzaley, & D'Esposito, 2004).

Single-trial estimation of LPP

EEG data from channel Pz was subject to ERP single trial estimation (Liu, Huang, McGinnis-Deweese, Keil, & Ding, 2012) using the Analysis of Single-trial ERP and Ongoing activity (ASEO) method (Xu, et al., 2009). Briefly, single trial EEG data are modeled as comprised of two parts: ERP and ongoing activity. The ERP part contains multiple components whose amplitude and latency vary from trial to trial. The ongoing activity part is assumed to be an autoregressive stochastic process. Based on this model, ASEO estimates single trial ERPs using an iterative maximum likelihood approach. The magnitude of the LPP for that trial was measured as the mean amplitude at Pz, between 400 and 800 ms post stimulus. These LPP amplitude estimates from each subject were then used to sort the trials and divide them into high and low LPP trials within either pleasant or unpleasant image categories using median split.

A median split was preferred over alternative methods such as quartiles or tertiles, as it maximized the number of trials included in the analysis, thereby enhancing statistical power. An additional advantage of the median split in this small sample of observers is that it enables a face (quasi-split-half) reliability check: Reliable network composition across halves of trials would be supported by the finding that networks (both appetitive and aversive) for high versus low LPP trials differ in strength and extent but not in the gross composition of regions. Using LPP single trial amplitudes to quantify the emotional intensity for each trial instead of self-report (affective ratings) affords a measure that is not bounded by an (ordinal) rating scale, can be objectively measured, can vary freely with multiple exposure to the same picture, and more directly reflects the brain processes mediating emotional engagement, compared to affective ratings.

Statistical inference

Two classes of group level random-effects analyses were conducted via paired t-tests on the Z-transformed correlation maps of individual subjects: (1) pleasant versus neutral scenes and unpleasant versus neutral scenes (valence contrast) and (2) high LPP group versus neutral

and low LPP group versus neutral within either pleasant or unpleasant image category (intensity contrast). Given the high number of trials in this paradigm, power to detect medium effects at the participant level was high, whereas fmripower software (see Mumford, 2012) indicated that only large effects could be detected at the group level, at a power of 80%, which is considered acceptable but not high (Desmond & Glover, 2002). To establish the extent to which the findings reported in this small-sample exploratory study are robust, we conducted several additional control analyses, including re-testing effects with split-half versions of the experiment, testing effects of the trial number included in each comparison, assessing the choice of seed region, and quantifying the risk for false positive results, by including control regions. The statistical threshold for all second-level analyses was set at $p < .05$ corrected for false discovery rate (FDR). For the valence contrast, clusters containing more than 10 significant contiguous voxels are shown. For the intensity contrast, because of reduced statistical power owing to smaller numbers of trials used, clusters containing more than 5 contiguous significant voxels are shown.

Results

MPFC-seeded correlation maps

Contrasting pleasant versus neutral scenes showed increased functional connectivity between the mPFC and higher-order executive structures and motor control areas (Figure 1A), including bilateral dorsolateral prefrontal cortex, supplementary motor area, anterior cingulate cortex, and left orbitofrontal cortex. Furthermore, mPFC interacted with the left calcarine sulcus and several extrastriate visual cortical areas such as the left cuneus, lingual gyrus, and superior occipital regions. Several regions associated with attention and perception were also functionally coupled with the mPFC during pleasant scene viewing, including the superior and inferior parietal cortex, fusiform gyrus, and the temporal pole. Regions associated with emotion-related mobilization for action showed strong appetitive mPFC connectivity, including the bilateral amygdala, hippocampus, as well as the precentral and postcentral gyri. Strikingly, there was no increase in functional connectivity between mPFC and other brain regions when conditions unpleasant and neutral were contrasted (Figure 1B), consistent with the hypothesis that mPFC centered networks exhibit specificity to appetitive content. Table 1 lists the regions exhibiting heightened mPFC-linked connectivity during emotional scene viewing.

Amygdala-seeded correlation maps

For the pleasant versus neutral contrast, amygdala exhibited increased connectivity with the left orbitofrontal cortex, bilateral dorsolateral prefrontal cortices, as well as areas in the extended visual cortex along the ventral stream, including left peri-calcarine, right precuneus and left cuneus, and the right inferior temporal gyrus (Figure 2A). Additional regions in the connectivity map included the caudate, the anterior cingulate cortex, left insula, and hippocampus. Contrasting unpleasant versus neutral viewing (Figure 2B) revealed a much broader network of areas that exhibited increased functional connectivity with the amygdala including striate and extrastriate visual cortices, areas in the temporal lobe (superior/middle/inferior temporal gyrus), and areas in dorsolateral prefrontal cortices, orbitofrontal cortex, and parietal cortices. Thalamus, hippocampus, parahippocampal gyrus, insula, anterior

cingulate cortex, motor cortices, and somatosensory cortices exhibited heightened interaction with the amygdala during aversive processing. From Table 2 the number of regions exhibiting increased amygdala connectivity during the viewing of unpleasant scenes is more than twice that during the viewing of pleasant pictures. These findings, consistent with our hypothesis, provide large-scale network evidence supporting the notion that amygdala forms distinct profiles of functional links with motive-specific brain regions during appetitive and aversive processing.

LPP-defined correlation maps

To examine whether seed-based functional connectivity is modulated by the intensity of emotional engagement, we used single-trial LPP amplitudes estimated from simultaneously recorded EEG as an index to divide the trials within a picture category into two groups of trials: large and small LPP amplitudes. The large and small LPP trials from pleasant and unpleasant categories were then separately contrasted against the trials from the neutral category. Results from these analyses were followed up by control analyses using randomly selected 50% of trials from the neutral category, to control for any spurious effects related to signal-to-noise differences in the LPP-based contrasts, which used only half of the trials (high or low LPP) in each comparison.

Regarding the mPFC-seeded correlation maps during the viewing of pleasant scenes, the present analyses demonstrated associations between trials with large LPP amplitudes and network interactions involving precentral/postcentral gyri which were often associated with emotion-related mobilization for action (Figure 3A). Functional connectivity also extended to the fusiform gyrus associated with higher-level visual processing and perception and the anterior cingulate cortex related to the modulation of emotional responses. Additional regions in the connectivity map included the supplementary motor area, middle/inferior temporal cortices and right occipital cortex. Note that the abovementioned structures remained significant in analyses in which only random subsets of neutral trials were used, to equate the number of neutral and pleasant trials used. By contrast, the mPFC-seeded correlation maps showed no significant interactions in trials with small LPP amplitudes, suggesting that the formation of large-scale networks reflects the extent of emotional engagement (Figure 3B). Mirroring our previous analyses, there was no increase in mPFC mediated functional connectivity during the viewing of unpleasant scenes, regardless of LPP amplitude (Figure 3C and 3D). This observation, together with Figure 1B, provides further support for the notion that mPFC forms a key component in a broadly distributed network that responds selectively to appetitive stimuli. Table 3 lists the regions with increased mPFC functional connectivity during emotional scene viewing, separately for the large and small LPP groups.

The amygdala-seeded connectivity map during viewing of pleasant scenes included the right temporal pole and left dorsolateral prefrontal cortex for trials with large LPP amplitudes (Figure 4A); it contained no regions for trials with small LPP amplitudes (Figure 4B). During the viewing of unpleasant scenes, the amygdala-seeded functional connectivity maps for the large LPP group (Figure 4C) contained large portions of the striate and extrastriate visual cortices, temporal lobe structures, as well as higher-order executive structures

including the dorsolateral prefrontal cortex, orbitofrontal cortex, and anterior cingulate cortex. Bilateral insula, left parietal cortex, left hippocampus, left parahippocampal gyrus, anterior cingulate cortex motor cortex, and somatosensory cortex also exhibited heightened interaction with the amygdala during more intense aversive processing. Again, this overall pattern structures remained significant in analyses in which only random subsets of neutral trials were used, to equate the number of neutral and pleasant trials used. A small subset (Figure 4D) of these areas remained in the amygdala-seeded correlation map when examining trials with small LPP amplitudes. Table 4 lists the regions that exhibited increased functional connectivity with the amygdala during the viewing of pleasant and unpleasant scenes separately for the large and small LPP trials.

Finally, concerns may arise from the repeated presentation of pictures across five blocks. A control analysis comparing the above connectivity maps for early versus late trials was conducted as an added control. These analyses resulted in no significant regions for the difference maps (early versus late), suggesting that the data from the first block are statistically equivalent to the data from subsequent blocks. Given the small sample, a further control analysis was conducted to quantify sensitivity/specificity of the beta-series analyses, using the auditory cortex as a seed region for the main comparisons conducted. These analyses support the specificity of the results for mPFC and amygdala seeds, as only one region (cuneus) in one of the comparisons (pleasant versus neutral) was connected to auditory cortex. Given previous reports on audiovisual attention capture during picture viewing (Keil et al., 2007), this specific region may be conceptually explained in a post-hoc fashion, but such a discussion is outside the scope of the present report. The fact however that none of the structures reported above were identified in this control analysis highlights the specificity and robustness of the beta-series method in the present sample.

Discussion

Viewing emotional pictures leads to heightened hemodynamic responses in a host of brain areas (Sabatinelli, et al., 2011). Past work has mainly focused on characterizing the co-activation of these areas. Here we aimed to map distributed interaction patterns among brain areas during exposure to natural scenes depicting pleasant, neutral, and unpleasant content. Motivated by the hypothesis that different coalitions of brain regions are assembled into large-scale networks depending on the motive system being engaged (e.g., appetitive vs. aversive), we first correlated single-trial beta values for each of the three picture categories. This approach allowed us to uncover distinct large-scale functional connectivity profiles by revealing the amount of correlated hemodynamic activity between core emotion processing structures (such as the amygdaloid complex and mPFC) and extended brain regions involved in perceptual-motor processing, memory and behavioral control. To further assess the modulation of these correlations by emotional intensity, we used single trial LPP from the simultaneously recorded EEG to index the varying intensity of emotional engagement within a hedonic valance and examined functional connectivity separately for large LPP trials and small LPP trials.

MPFC and its functional connectivity

The mPFC was hypothesized to be the core component of a large-scale network sensitive to appetitive processing, important for coordinating sensory and motor areas to support amplified sensory processing and response mobilization towards appetitive cues (Price, 1999). The present functional connectivity analyses are consistent with evidence from previous studies that mPFC networks exhibit preferential recruitment during appetitive processing (Costa, Lang, Sabatinelli, Versace, & Bradley, 2010; Sabatinelli, Bradley, Lang, Costa, & Versace, 2007; Sabatinelli, Flaisch, Bradley, Fitzsimmons, & Lang, 2004). In a previous study with the same data (Liu et al., 2012), the LPP amplitude elicited by pleasant pictures co-varied with BOLD in the mPFC, occipitotemporal junction, amygdala, and precuneus. In the present study, the mPFC-mediated appetitive network included widespread cortical regions involved in visual processing (ventral visual stream) and action selection, in addition to numerous deep brain regions such as the hippocampal, amygdaloid complexes and the ACC, responsible for memory and cognitive control. By contrast, our analyses revealed no mPFC-linked areas that were preferentially engaged during the processing of aversive stimuli. These findings support the existence of a unique and dedicated mPFC-mediated functional neural organization for appetitive processing. The absence of mPFC-related connectivity in the unpleasant condition strongly suggests that the appetitive network outlined above (Figure 1 and Table 1) is not driven by stimulus salience or general arousal.

Previous research suggests the nucleus accumbens (NAcc) plays an important role in appetitive engagement during both pleasant scene viewing (Costa, Lang, Sabatinelli, Versace, & Bradley, 2010; Sabatinelli, Lang, Bradley, Costa, & Keil, 2009) and pleasant imagery (Costa, Lang, Sabatinelli, Versace, & Bradley, 2010). In the present study, NAcc was contained only in the mPFC-seeded correlation maps for pleasant versus neutral contrast under a relaxed threshold ($p<0.07$ FDR). Using the NAcc seed identified by contrasting BOLD evoked by pleasant and neutral pictures (Liu et al., 2012), no areas appeared in the corresponding correlation maps under $p < .05$ FDR. Using the NAcc seed identified in a previous study (Heldmann, et al., 2012; MNI coordinates: [10,12,-2] and [−10,12,-2]), the corresponding correlation maps revealed three small regions under $p < .05$ FDR (the caudate, a section of the superior medial frontal cortex, and the precuneus) when comparing pleasant and neutral content. Together, these findings suggest that mPFC is the main valence-sensitive region for coordinating a network of areas involved in perceiving and mobilizing action in response to pleasant motivational affordances. As noted in the Methods, the fact that pleasantness ratings for neutral pictures were relatively high may have diminished the contrast for connectivity during pleasant picture viewing. This methodological constraint may further explain differences between the findings of the present study and previous work addressing connectivity during pleasant picture viewing: For example, work interested in cognitive aging, emotional memory, or emotional distraction (Addis, Leclerc, Muscatell, & Kensinger, 2010; Allard & Kensinger, 2014; Iordan & Dolcos, 2015) has identified widespread connectivity of mPFC with frontal cortical structures considered part of the central executive or default mode networks (Bressler & Menon, 2010). In addition to differences in stimulus material, it is likely that the use of memory and distraction paradigms as opposed to the passive viewing situation employed here has

contributed to divergent results between the present exploration and the work mentioned above.

The amygdala and its functional connectivity

Our findings support the hypothesis that amygdala established connections with different brain regions depending on the hedonic valence of the system being engaged. Amygdala-seeded coupling during appetitive processing was restricted to the visual cortex as well as areas involved in attention and executive function (e.g., precuneus) and in the encoding of hedonic value such as the caudate and insula (Naqvi & Bechara, 2010; Phan, Wager, Taylor, & Liberzon, 2002). During aversive processing, connections were stronger and more widespread between the bilateral amygdala and visual cortex. In addition, our findings suggest a unique profile of amygdala-seeded functional connectivity during the processing of aversive scenes, characterized by involvement of the superior/middle temporal gyrus, superior/inferior parietal cortex, the cingulate cortex, and supplementary motor area, along with critical subcortical structures including the thalamus, hippocampus, and insula. These regions, including perceptual and motor areas as well as cortical regions involved in executive and memory processing, correspond largely with previous studies examining beta-series connectivity when observers view IAPS pictures (e.g., St. Jacques, Dolcos, & Cabeza, 2010). The formation of such function-dependent flexible links between the amygdaloid body and other structures during specific motivational and behavioral conditions is in line with research in animal models (Salzman, Paton, Belova, & Morrison, 2007).

A previous study on the same data set (Liu et al., 2012) used trial-by-trial correlation of LPP amplitude and BOLD, separately for pleasant and unpleasant pictures, to identify brain regions co-varying with emotional engagement. Analyses of EEG-BOLD coupling identify brain regions in which spatially low-pass filtered post-synaptic neural processes (the EEG-derived signal) and BOLD co-vary, thus highlighting regionally specific hemodynamic changes that predict spatially non-specific neuro-electric changes. Thus, the beta-series method used here (which highlights brain areas displaying systematic BOLD co-variation across time) is more spatially specific than the LPP-BOLD coupling analysis, reflected in spatially richer results compared to Liu et al., (2012). This may be unsurprising given the less spatially specific nature of EEG signals (Nunez & Srinivasan, 2006). Differences between the two studies are therefore informative regarding the type of information that may be reflected by scalp-recorded EEG/ERP signals: Both studies suggested coupling between motivational hubs and sensory and motor cortex, along with ACC and insular cortex connectivity. This suggests that late scalp-recorded ERP signals such as the LPP may be sensitive to activity in wide-spread brain networks of coherently active brain regions, and that these networks may overlap with those identified by BOLD connectivity measures. Future work may systematically examine the relation between BOLD connectivity and different measures of scalp-recorded electrophysiology collected during emotional perception.

Our findings support the notion that the function of a given brain region is an emergent phenomenon that depends on its participation within broadly distributed brain networks rather than being an isolated property of neural tissue (Pessoa, 2014; Singer, 2013). For

example, while numerous findings suggest that general emotional arousal enhances BOLD responses in the amygdaloid complex (Lang & Bradley, 2010), the pattern of broad network interactions appears to exhibit motive system specificity. Indeed, a conventional fMRI activation analysis of the present BOLD data via GLM showed that amygdala was active for both unpleasant and pleasant pictures (Liu, Huang, McGinnis-Deweese, Keil, & Ding, 2012). Yet, amygdala-seeded connectivity suggests that this region establishes flexible interactions with other brain regions and both the anatomical specificity and breadth of these interactions differ for aversive versus appetitive processing. Recent work assessing large-scale BOLD connectivity in terms of established networks (e.g., Bressler & Menon, 2010) found that ventral regions, including deep medial temporal structures such as the amygdaloid body, tend to be part of (or tightly linked to) structures in the so-called salience network (Seeley et al., 2007), which is organized around fronto-insular cortex and the ACC (Touroutoglou et al., 2014). As discussed in Iordan & Dolcos (2015), these structures may form task-dependent links with other established networks such as the executive control network (Seeley et al., 2007), or structures contained in the default-mode network (Raichle et al., 2001). Specifically, the mPFC (often considered part of the default network) has been reported to display coupling with the amygdaloid complex and adjacent structures during distraction with unpleasant visual stimuli, while at the same time also displaying heightened connectivity with structures thought to mediate executive control (Iordan & Dolcos, 2015).

Emotional modulation of visual processing

A consistent finding is that both the mPFC-seeded appetitive network and amygdala-seeded appetitive and aversive networks included visual cortices in the current study. In particular, large portions of the ventral stream coalesced into assemblies established around valence-sensitive brain areas. This observation provides support for the re-entry hypothesis of emotional perception. Stated generally, the re-entry hypothesis predicts that emotion-sensitive core structures engage sensory areas through feedback connections, facilitating the perceptual processing of emotionally salient stimuli (Keil et al., 2009). Although the present data are limited in that they do not reflect directional information flow among brain regions, the bi-directional communication associated with re-entry is consistent with the coupling observed in the current study.

Functional connectivity and intensity of emotional engagement

Considerable evidence suggests that LPP amplitude is associated with the degree of emotional arousal (Cuthbert, Schupp, Bradley, Birbaumer, & Lang, 2000; Hajcak, MacNamara, & Olvet, 2010; Keil, et al., 2002; Liu, Huang, McGinnis-Deweese, Keil, & Ding, 2012). LPP amplitude to neutral scenes correlates with self-reported emotional arousal. LPP amplitude to affective scenes has been used to index the intensity of emotional engagement (Keil et al., 2002). The mPFC-seeded appetitive network and the amygdala-seeded appetitive and aversive networks were computed using single-trial LPP amplitude estimates, to identify the relation between the level of LPP amplitude estimates and seed-based functional connectivity in the brain. Considerable overlap was observed between connectivity maps based on trials with low and high LPP amplitude, which supports the reliability of the beta series method, but the extent of high-LPP networks tended to be larger. Thus, our findings support the hypothesis that the strength of functional interactions between

hub regions such as amygdala and mPFC and other brain areas is positively associated with the intensity of emotional processing. This in turn suggests that the LPP provides a surface electrophysiological correlate of activation in and interaction among broadly distributed brain networks (Liu, Huang, McGinnis-Deweese, Keil, & Ding, 2012; Moratti, Saugar, & Strange, 2011; Sabatinelli, Keil, Frank, & Lang, 2013). It is worth noting that Tables 3 and 4 contained fewer areas than Tables 1 and 2, potentially reflecting weakened statistical power due to reduced numbers of trials.

Conclusions

Taken together, the present data converge with animal and human findings (Keil, et al., 2012), to demonstrate that appetitive and aversive stimulus processing are associated with heightened coupling between core affective structures and an array of brain areas associated with sensory and motor processing as well as executive control . In line with motivational and evolutionary theories of affect, emotion networks in the brain may link perceptual features reliably paired with threat or reward to support attentive behavior and ultimately mediate the preparation of the organism for goal-oriented adaptive action. Although the networks emerging in response to different emotional challenges share individual components, the specific nature of motive system engagement is reflected in the distinct forms of functional coupling of varying structures into large-scale brain networks.

Acknowledgements

This work was supported by NIH grant MH097320. The authors would like to thank Nina Thigpen for valuable comments on an earlier draft of this manuscript.

References

Addis DR, Leclerc CM, Muscatell KA, Kensinger EA. There are age-related changes in neural connectivity during the encoding of positive, but not negative, information. Cortex. 2010; 46(4): 425–433. doi: 10.1016/j.cortex.2009.04.011. [PubMed: 19555933]

Allard ES, Kensinger EA. Age-Related Differences in Functional Connectivity During Cognitive Emotion Regulation. The Journals of Gerontology Series B: Psychological Sciences and Social Sciences. 2014; 69(6):852–860. doi: 10.1093/geronb/gbu108.

Allen PJ, Josephs O, Turner R. A Method for Removing Imaging Artifact from Continuous EEG Recorded during Functional MRI. Neuroimage. 2000; 12:230–239. doi: 10.1006/nimg.2000.0599. [PubMed: 10913328]

Allen PJ, Polizzi G, Krakow K, Fish DR, Lemieux L. Identification of EEG Events in the MR Scanner: The Problem of Pulse Artifact and a Method for Its Subtraction. Neuroimage. 1998; 8:229–239. doi: 10.1006/nimg.1998.0361. [PubMed: 9758737]

Axmacher N, Schmitz DP, Wagner T, Elger CE, Fell J. Interactions between medial temporal lobe, prefrontal cortex, and inferior temporal regions during visual working memory: a combined intracranial EEG and functional magnetic resonance imaging study. J Neurosci. 2008; 28:7304–7312. doi: 10.1523/JNEUROSCI.1778-08.2008. [PubMed: 18632934]

Belouchrani A, Abed-Meraim K, Cardoso JF, Moulines E. Second-order blind separation of temporally correlated sources. Proc Int Conf on Digital Sig Proc. 1993:346–351.

Bradley MM. Natural selective attention: orienting and emotion. Psychophysiology. 2009; 46:1–11. doi: 10.1111/j.1469-8986.2008.00702.x. [PubMed: 18778317]

Bradley MM, Costa VD, Ferrari V, Codispoti M, Fitzsimmons JR, Lang PJ. Imaging distributed and massed repetitions of natural scenes: spontaneous retrieval and maintenance. Hum Brain Mapp.

2015; 36:1381–1392. doi: 10.1002/hbm.22708. doi: 10.1016/0005-7916(94)90063-9. [PubMed: 25504854]

Bradley MM, Lang PJ. Measuring emotion: the Self-Assessment Manikin and the Semantic Differential. J Behav Ther Exp Psychiatry. 1994; 25:49–59. [PubMed: 7962581]

Bressler SL, Menon V. Large-scale brain networks in cognition: emerging methods and principles. Trends in Cognitive Sciences. 2010; 14(6):277–290. doi: 10.1016/j.tics.2010.04.004. [PubMed: 20493761]

Chadick JZ, Gazzaley A. Differential coupling of visual cortex with default or frontal-parietal network based on goals. Nat Neurosci. 2011; 14:830–832. doi: 10.1038/nn.2823. [PubMed: 21623362]

Codispoti M, Ferrari V, Bradley MM. Repetitive picture processing: Autonomic and cortical correlates. Brain Research. 2006; 1068(1):213–220. doi: 10.1016/j.brainres.2005.11.009. [PubMed: 16403475]

Costa VD, Lang PJ, Sabatinelli D, Versace F, Bradley MM. Emotional imagery: assessing pleasure and arousal in the brain's reward circuitry. Hum Brain Mapp. 2010; 31:1446–1457. doi: 10.1002/hbm.20948. [PubMed: 20127869]

Cuthbert BN, Schupp HT, Bradley MM, Birbaumer N, Lang PJ. Brain potentials in affective picture processing: covariation with autonomic arousal and affective report. Biol Psychol. 2000; 52:95–111. doi: 10.1016/S0301-0511(99)00044-7. [PubMed: 10699350]

Delorme A, Makeig S. EEGLAB: an open source toolbox for analysis of single-trial EEG dynamics including independent component analysis. J Neurosci Methods. 2004; 134:9–21. doi: 10.1016/j.jneumeth.2003.10.009. [PubMed: 15102499]

Desmond JE, Glover GH. Estimating sample size in functional MRI (fMRI) neuroimaging studies: Statistical power analyses. Journal of Neuroscience Methods. 2002; 118(2):115–128. doi: 10.1016/S0165-0270(02)00121-8. [PubMed: 12204303]

Fan J, Gu X, Liu X, Guise KG, Park Y, Martin L, de Marchena A, Tang CY, Minzenberg MJ, Hof PR. Involvement of the anterior cingulate and frontoinsular cortices in rapid processing of salient facial emotional information. Neuroimage. 2011; 54:2539–2546. doi: 10.1016/j.neuroimage.2010.10.007. [PubMed: 20937394]

Ferrari V, Bradley MM, Codispoti M, Lang PJ. Repetitive exposure: Brain and reflex measures of emotion and attention. Psychophysiology. 2011; 48(4):515–22. doi: 10.1111/j.1469-8986.2010.01083.x. [PubMed: 20701711]

Hajcak G, MacNamara A, Olvet DM. Event-related potentials, emotion, and emotion regulation: an integrative review. Dev Neuropsychol. 2010; 35:129–155. doi: 10.1080/87565640903526504. [PubMed: 20390599]

Hayes DJ, Northoff G. Identifying a network of brain regions involved in aversion-related processing: a cross-species translational investigation. Front Integr Neurosci. 2011; 5:49. doi: 10.3389/fnint.2011.00049. [PubMed: 22102836]

Heldmann M, Berding G, Voges J, Bogerts B, Galazky I, Muller U, Baillot G, Heinze HJ, Munte TF. Deep brain stimulation of nucleus accumbens region in alcoholism affects reward processing. PLoS One. 2012; 7:e36572. doi: 10.1371/journal.pone.0036572. [PubMed: 22629317]

Iordan AD, Dolcos F. Brain Activity and Network Interactions Linked to Valence-Related Differences in the Impact of Emotional Distraction. Cerebral Cortex. 2015:bhv242. doi: 10.1093/cercor/bhv242. [PubMed: 26543041]

Keil A, Bradley MM, Hauk O, Rockstroh B, Elbert T, Lang PJ. Large-scale neural correlates of affective picture processing. Psychophysiology. 2002; 39:641–649. doi: 10.1111/1469-8986.3950641. [PubMed: 12236331]

Keil A, Bradley MM, Junghoefer M, Russmann T, Lowenthal W, Lang PJ. Cross-modal Attention Capture by Affective Stimuli: Evidence from Event-Related Potentials. Cognitive, Affective, & Behavioral Neuroscience. 2007; 7(1):18–24. doi: 10.3758/CABN.7.1.18.

Keil A, Costa V, Smith JC, Sabatinelli D, McGinnis EM, Bradley MM, Lang PJ. Tagging cortical networks in emotion: a topographical analysis. Hum Brain Mapp. 2012; 33:2920–2931. doi: 10.1002/hbm.21413. [PubMed: 21954087]

Keil A, Sabatinelli D, Ding M, Lang PJ, Ihssen N, Heim S. Re-entrant Projections Modulate Visual Cortex in Affective Perception: Directional Evidence from Granger Causality Analysis. Human Brain Mapping. 2009; 30:532–540. doi: 10.1002/hbm.20521. [PubMed: 18095279]

Kinnison J, Padmala S, Choi JM, Pessoa L. Network analysis reveals increased integration during emotional and motivational processing. J Neurosci. 2012; 32:8361–8372. doi: 10.1523/JNEUROSCI.0821-12.2012. [PubMed: 22699916]

Lang PJ, Bradley MM. Emotion and the motivational brain. Biol Psychol. 2010; 84:437–450. doi: 10.1016/j.biopsycho.2009.10.007. [PubMed: 19879918]

Lang, PJ.; Bradley, MM.; Cuthbert, BN. International affective picture system (IAPS): Affective ratings of pictures and instruction manual. Technical Report A-8. University of Florida; Gainesville, FL: 2008.

LeDoux J. Rethinking the emotional brain. Neuron. 2012; 73:653–676. doi: 10.1016/j.neuron.2012.02.004. [PubMed: 22365542]

Lindquist KA, Wager TD, Kober H, Bliss-Moreau E, Barrett LF. The brain basis of emotion: a meta-analytic review. Behav Brain Sci. 2012; 35:121–143. doi: 10.1017/S0140525X11000446. [PubMed: 22617651]

Liu Y, Huang H, McGinnis-Deweese M, Keil A, Ding M. Neural substrate of the late positive potential in emotional processing. J Neurosci. 2012; 32:14563–14572. doi: 10.1523/JNEUROSCI.3109-12.2012. [PubMed: 23077042]

Miskovic V, Martinovic J, Wieser MJ, Petro NM, Bradley MM, Keil A. Electrocortical amplification for emotionally arousing natural scenes: The contribution of luminance and chromatic visual channels. Biological Psychology. 2015; 106:11–17. doi: 10.1016/j.biopsycho.2015.01.012. [PubMed: 25640949]

Moran TP, Jendrusina AA, Moser JS. The psychometric properties of the late positive potential during emotion processing and regulation. Brain Research. 2013; 1516:66–75. doi: 10.1016/j.brainres.2013.04.018. [PubMed: 23603408]

Moratti S, Saugar C, Strange BA. Prefrontal-occipitoparietal coupling underlies late latency human neuronal responses to emotion. J Neurosci. 2011; 31:17278–17286. doi: 10.1523/JNEUROSCI.2917-11.2011. [PubMed: 22114294]

Mumford JA. A power calculation guide for fMRI studies. Social Cognitive and Affective Neuroscience. 2012:nss059. doi: 10.1093/scan/nss059.

Nagahama Y, Okada T, Katsumi Y, Hayashi T, Yamauchi H, Sawamoto N, Toma K, Nakamura K, Hanakawa T, Konishi J, Fukuyama H, Shibasaki H. Transient neural activity in the medial superior frontal gyrus and precuneus time locked with attention shift between object features. Neuroimage. 1999; 10:193–199. doi: 10.1006/nimg.1999.0451. [PubMed: 10417251]

Naqvi NH, Bechara A. The insula and drug addiction: an interoceptive view of pleasure, urges, and decision-making. Brain Struct Funct. 2010; 214:435–450. doi: 10.1007/s00429-010-0268-7. [PubMed: 20512364]

Nunez, PL.; Srinivasan, R. Electric fields of the brain. 2nd ed.. Oxford University Press; New York, NY: 2006. doi: 10.1093/acprof:oso/9780195050387.001.0001

Pessoa L. Understanding brain networks and brain organization. Physics of Life Reviews. 2014; 11:400–435. doi: 10.1016/j.plrev.2014.03.005. [PubMed: 24819881]

Pessoa L, Adolphs R. Emotion processing and the amygdala: from a ‘low road’ to ‘many roads’ of evaluating biological significance. Nat Rev Neurosci. 2010; 11:773–783. doi: 10.1038/nrn2920. [PubMed: 20959860]

Phan KL, Wager T, Taylor SF, Liberzon I. Functional neuroanatomy of emotion: a meta-analysis of emotion activation studies in PET and fMRI. Neuroimage. 2002; 16:331–348. doi: 10.1006/nimg.2002.1087. [PubMed: 12030820]

Price JL. Prefrontal cortical networks related to visceral function and mood. Ann N Y Acad Sci. 1999; 877:383–396. doi: 10.1111/j.1749-6632.1999.tb09278.x. [PubMed: 10415660]

Raichle ME, MacLeod AM, Snyder AZ, Powers WJ, Gusnard DA, Shulman GL. A default mode of brain function. Proceedings of the National Academy of Sciences. 2001; 98(2):676–682. doi: 10.1073/pnas.98.2.676.

Rissman J, Gazzaley A, D'Esposito M. Measuring functional connectivity during distinct stages of a cognitive task. Neuroimage. 2004; 23:752–763. doi: 10.1016/j.neuroimage.2004.06.035. [PubMed: 15488425]

Rissman J, Gazzaley A, D'Esposito M. Dynamic adjustments in prefrontal, hippocampal, and inferior temporal interactions with increasing visual working memory load. Cereb Cortex. 2008; 18:1618–1629. doi: 10.1093/cercor/bhm195. [PubMed: 17999985]

Sabatinelli D, Bradley MM, Lang PJ, Costa VD, Versace F. Pleasure rather than salience activates human nucleus accumbens and medial prefrontal cortex. J Neurophysiol. 2007; 98:1374–1379. doi: 10.1152/jn.00230.2007. [PubMed: 17596422]

Sabatinelli D, Flaisch T, Bradley MM, Fitzsimmons JR, Lang PJ. Affective picture perception: gender differences in visual cortex? Neuroreport. 2004; 15:1109–1112. doi: 10.1097/00001756-200405190-00005. [PubMed: 15129155]

Sabatinelli D, Fortune EE, Li Q, Siddiqui A, Krafft C, Oliver WT, Beck S, Jeffries J. Emotional perception: meta-analyses of face and natural scene processing. Neuroimage. 2011; 54:2524–2533. doi: 10.1016/j.neuroimage.2010.10.011. [PubMed: 20951215]

Sabatinelli D, Keil A, Frank DW, Lang PJ. Emotional perception: correspondence of early and late event-related potentials with cortical and subcortical functional MRI. Biol Psychol. 2013; 92:513–519. doi: 10.1016/j.biopsycho.2012.04.005. [PubMed: 22560889]

Sabatinelli D, Lang PJ, Bradley MM, Costa VD, Keil A. The timing of emotional discrimination in human amygdala and ventral visual cortex. J Neurosci. 2009; 29:14864–14868. doi: 10.1523/JNEUROSCI.3278-09.2009. [PubMed: 19940182]

Sabatinelli D, Lang PJ, Keil A, Bradley MM. Emotional perception: correlation of functional MRI and event-related potentials. Cereb Cortex. 2007; 17:1085–1091. doi: 10.1093/cercor/bhl017. [PubMed: 16769742]

Salzman CD, Paton JJ, Belova MA, Morrison SE. Flexible neural representations of value in the primate brain. Ann N Y Acad Sci. 2007; 1121:336–354. doi: 10.1196/annals.1401.034. [PubMed: 17872400]

Schupp HT, Cuthbert BN, Bradley MM, Hillman CH, Hamm AO, Lang PJ. Brain Processes in emotional perception: Motivated attention. Cognition and Emotion. 2004; 18:593–611. doi: 10.1080/02699930341000239.

Seeley WW, Menon V, Schatzberg AF, Keller J, Glover GH, Kenna H, Greicius MD. Dissociable Intrinsic Connectivity Networks for Salience Processing and Executive Control. The Journal of Neuroscience. 2007; 27(9):2349–2356. doi: 10.1523/JNEUROSCI.5587-06.2007. [PubMed: 17329432]

Seymour B, Singer T, Dolan R. The neurobiology of punishment. Nat Rev Neurosci. 2007; 8:300–311. doi: 10.1038/nrn2119. [PubMed: 17375042]

Singer W. Cortical dynamics revisited. Trends Cogn Sci. 2013; 17:616–626. doi: 10.1016/j.tics.2013.09.006. [PubMed: 24139950]

Swanson LW. Cerebral hemisphere regulation of motivated behavior. Brain Res. 2000; 886:113–164. doi: 10.1016/S0006-8993(00)02905-X. [PubMed: 11119693]

Touroutoglou A, Bickart KC, Barrett LF, Dickerson BC. Amygdala task-evoked activity and task-free connectivity independently contribute to feelings of arousal. Human Brain Mapping. 2014; 35(10):5316–5327. doi: 10.1002/hbm.22552. [PubMed: 24862171]

Xu L, Stoica P, Li J, Bressler SL, Shao X, Ding M. ASEO: a method for the simultaneous estimation of single-trial event-related potentials and ongoing brain activities. IEEE Trans Biomed Eng. 2009; 56:111–121. doi: 10.1109/TBME.2008.2008166. [PubMed: 19224725]

Young MP, Scannell JW, Burns GA, Blakemore C. Analysis of connectivity: neural systems in the cerebral cortex. Rev Neurosci. 1994; 5:227–250. doi: 10.1515/revneuro.1994.5.3.227. [PubMed: 7889215]

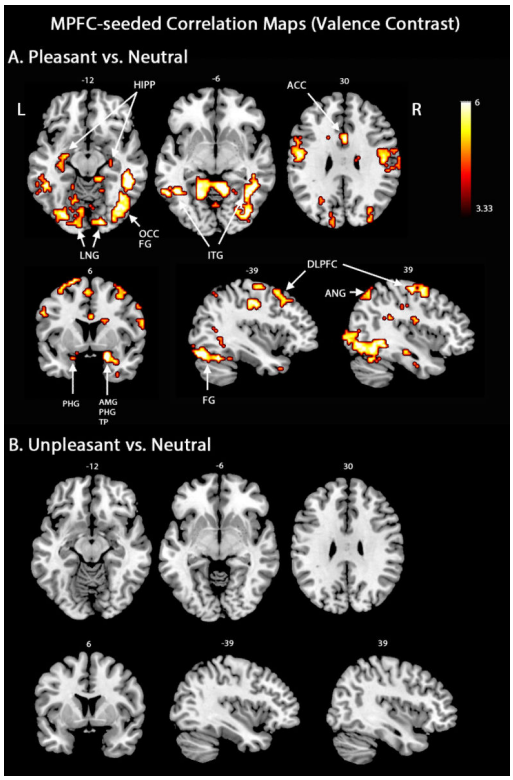

Figure 1.

MPFC-seeded beta-series correlation maps. A. An extensive network was connected to mPFC when pleasant and neutral picture viewing were contrasted. B. No region was connected to mPFC when pleasant and neutral picture viewing were contrasted. Map thresholds were set at $p < .05$ (FDR corrected). HIPP, hippocampus; LNG, lingual gyrus; OCC, occipital cortex; FG, fusiform gyrus; ITG, inferior temporal gyrus; ACC, anterior cingulate cortex; PHG, parahippocampal gyrus; AMG, amygdala; TP, temporal pole; DLFPC, dorsolateral prefrontal cortex; ANG, angular gyrus.

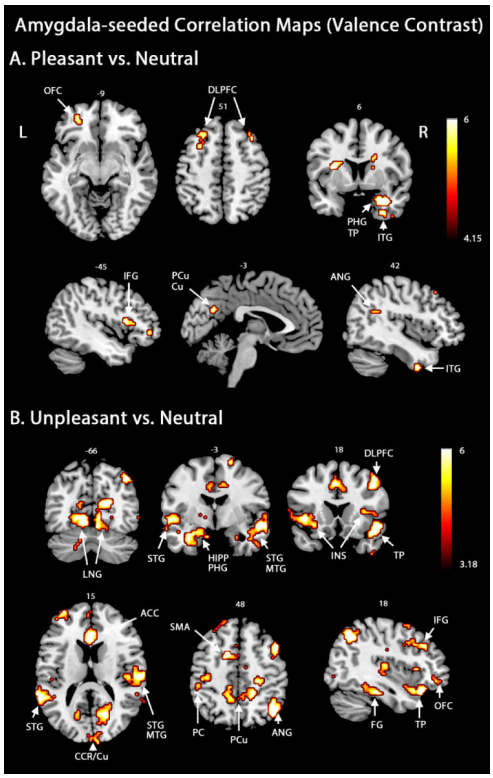

Figure 2.

Amygdala-seeded beta-series correlation maps. A. Regions connected to amygdala when pleasant picture viewing was contrasted against the neutral picture condition. B. Regions connected to the amygdala when unpleasant and neutral picture viewing were contrasted. Map thresholds were set at $p < .05$ (FDR corrected). OFC, orbitofrontal cortex; IFG, inferior frontal gyrus; PCu, precuneus; Cu, cuneus; STG, superior temporal gyrus; MTG, middle temporal gyrus; INS, insula; CCR, calcarine; SMA, supplementary motor area; PC, parietal cortex.

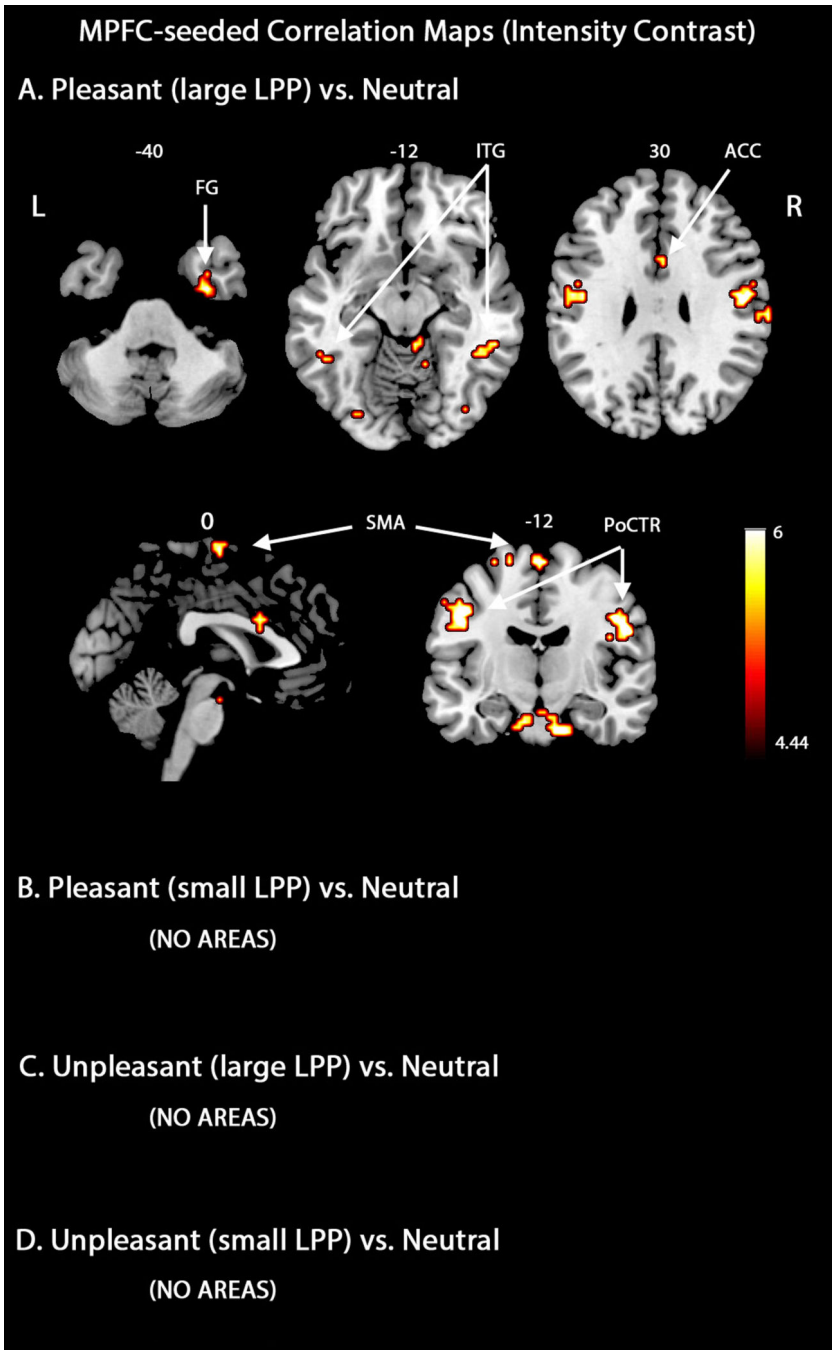

Figure 3.

MPFC-seeded beta-series correlation maps based on engagement intensity contrast. A. Regions connected to mPFC when pleasant and neutral picture viewing were contrasted (large LPP group). B. Regions connected to mPFC when conditions pleasant and neutral were contrasted (small LPP group). C-D. Regions connected to mPFC when conditions unpleasant and neutral were contrasted (large and small LPP groups). All map thresholds were set at $p < .05$ (FDR corrected). PoCTR, postcentral gyrus.

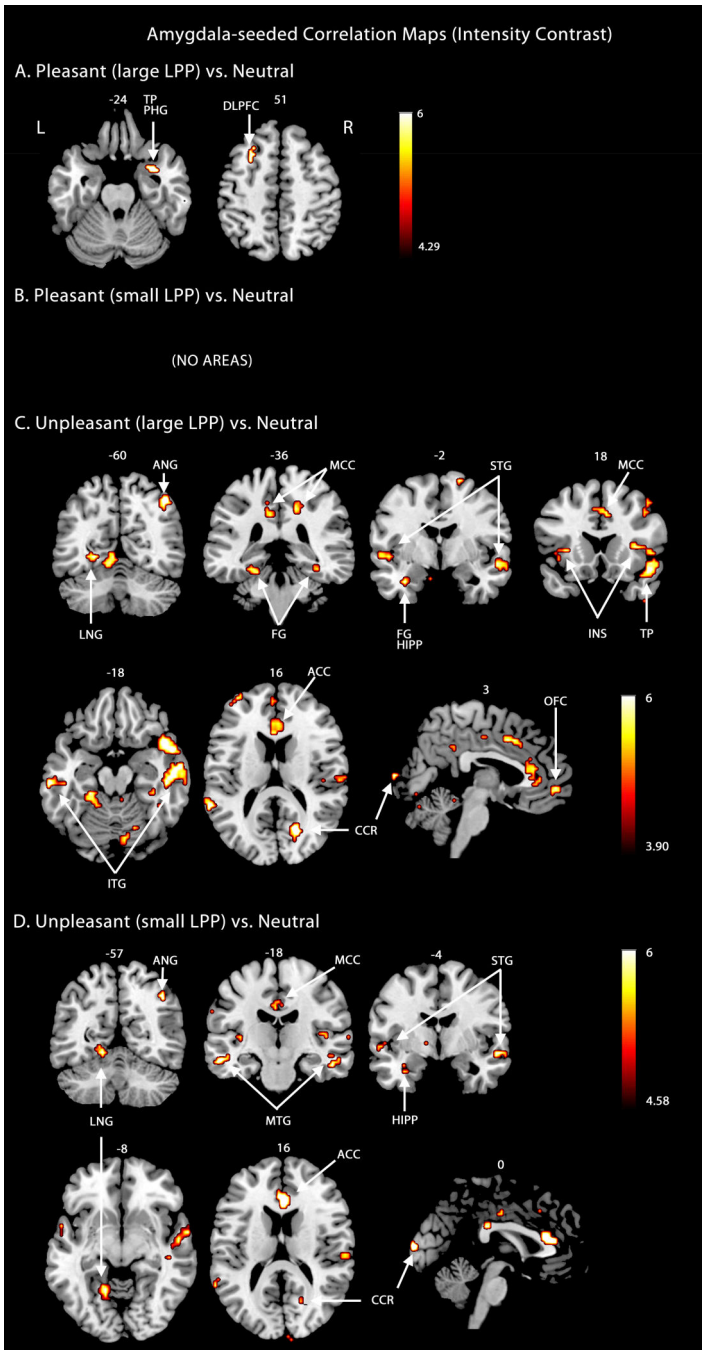

Figure 4.

Amygdala-seeded beta-series correlation maps based on engagement intensity contrast. A. Regions connected to amygdala when conditions pleasant and neutral were contrasted (large LPP group). B. Regions connected to amygdala conditions pleasant and neutral were contrasted (small LPP group). C. Regions connected to amygdala when conditions unpleasant and neutral were contrasted (large LPP group). D. Regions connected to

amygdala when conditions unpleasant and neutral were contrasted (small LPP group). All map thresholds were set at $p < .05$ (FDR corrected). MCC, middle cingulate cortex.

Table 1

Regions connected with mPFC during viewing of pleasant and unpleasant pictures.

Anatomical Regions	MNI coordinates x,y,z (Z score)	
	Pleasant pictures	Unpleasant pictures
Frontal		
Dorsolateral prefrontal cortex	−27, −6, 66 (4.65)	
	27, −9, 72 (4.45)	
Orbitofrontal cortex	−27, 30, −21 (3.54)	
Precentral gyrus	−18, −12, 69 (3.61)	
	63, 12, 18 (3.68)	
Supplementary motor area	0, −9, 66 (3.69)	
Temporal		
Middle temporal gyrus	−57, −36, −12 (2.81)	
Inferior temporal gyrus	−57, −42, −15 (3.92)	
	54, −45, −21 (4.33)	
Temporal pole	−36, 15, −36 (3.75)	
Parietal		
Superior parietal cortex	−30, −69, 54 (3.70)	
	21, −72, 51 (3.49)	
Inferior parietal cortex	−60, −36, 42 (3.33)	
Postcentral gyrus	−51, −9, 39 (4.31)	
	48, −12, 33 (4.11)	
Angular gyrus	−45, −63, 51 (3.00)	NO AREAS
	42, −66, 51 (3.32)	
Precuneus	−15, −57, 51 (4.73)	
Supramarginal gyrus	66, −24, 24 (3.61)	
Occipital		
Superior occipital cortex	−24, −66, 33 (3.09)	
	27, −66, 24 (3.54)	
Medial occipital cortex	−24, −81, 18 (3.38)	
	30, −78, 24 (3.37)	
Inferior occipital cortex	36, −72, −9 (4.26)	
Lingual gyrus	−18, −57, −3 (5.08)	
	12, −51, −6 (4.73)	
Calcarine	−21, −72, 12 (2.78)	
Subcortical		
Caudate	−18, 18, 18 (3.34)	
	21, 9, 24 (3.49)	
Anterior cingulate cortex	0, 12, 27 (4.25)	
Parahippocampal gyrus/Hippocampus	−27, −9, −15 (4.04)	
	21, 6, −21 (4.34)	

Table 2

Regions connected with amygdala during viewing of pleasant and unpleasant pictures.

Anatomical Regions	MNI coordinates x,y,z (Z score)	
	Pleasant pictures	Unpleasant pictures
Frontal		
Dorsolateral prefrontal cortex	−27, 33, 45 (4.30)	−42, 51, 18 (4.24)
	36, 24, 51 (4.59)	36, 30, 36 (4.36)
Orbitofrontal cortex	−27, 45, −6 (4.21)	
Orbitofrontal cortex		39, 27, −21 (5.33)
Inferior frontal gyrus	−51, 24, 12 (4.52)	
Inferior frontal gyrus		45, 15, 42 (4.77)
Precentral gyrus		−45, 6, 42 (3.43)
Precentral gyrus	33, −15, 69 (4.30)	45, 3, 42 (2.80)
Supplementary motor area		−3, −9, 63 (3.6)
Temporal		
Superior temporal gyrus		−63, −45, 18 (5.24)
		51, −9, −12 (5.04)
Middle temporal gyrus		−61, −45, 13 (3.87)
		55, −13, −18 (4.24)
Inferior temporal gyrus		−63, −24, −18 (4.41)
Inferior temporal gyrus	42, 3, −45 (3.93)	57, −18, −18 (5.48)
Temporal pole	30, 9, −27 (5.08)	48, 15, −18 (4.83)
Fusiform gyrus		−24, −33, −18 (4.42)
		36, −30, −21 (4.11)
Parietal		
Superior parietal cortex		−24, −48, 63 (3.83)
Inferior parietal cortex		−48, −36, 51 (3.55)
		42, −55, 50 (3.85)
Angular gyrus		42, −63, 45 (5.36)
Postcentral gyrus		−45, −24, 48 (3.60)
		51, −21, 33 (3.09)
Precuneus	−15, −42, 3 (3.65)	−15, −45, 45 (3.43)
Precuneus		15, −42, 42 (4.2)
Occipital		
Medial occipital cortex		−30, −90, 21 (3.64)
		42, −90, 0 (2.77)
Inferior occipital cortex		48, −81, −3 (3.62)
Lingual gyrus		−12, −66, 0 (4.64)
		6, −69, 0 (4.63)
Calcarine	−3, −64, 27 (3.19)	0, −99, 9 (4.34)
Cuneus	−6, −63, 27 (3.91)	
Subcortical		

Anatomical Regions	MNI coordinates x,y,z (Z score)	
	Pleasant pictures	Unpleasant pictures
Anterior cingulate cortex	18, 45, 6 (3.27)	3, 33, 15 (4.01)
Middle cingulate cortex		0, −15, 42 (3.72)
Posterior cingulate cortex		0, −39, 30 (3.92)
Parahippocampal gyrus/Hippocampus	−27, −33, −3 (3.78)	−33, −3, −27 (4.39)
	28, 9, −28 (4.39)	27, −3, −24 (3.35)
Insula	−33, 6, 15 (4.89)	−33, 21, −8 (3.93)
Insula		46, 20, −8 (3.72)
Caudate	−12, 24, 0 (3.55)	
	12, 15, 18 (3.63)	
Thalamus		−6, −9, 0 (4.37)
		6, −18, 3 (2.85)

Table 3

Regions connected with mPFC for large LPP trials and small LPP trials.

Anatomical Regions	MNI coordinates x,y,z (Z score)	
	Pleasant pictures	
	Large LPP	Small LPP
Frontal		
Precentral gyrus	−18, −12, 69 (3.90)	
	63, 12, 21 (4.22)	
Temporal		
Middle temporal gyrus	54, −39, −12 (3.90)	
Inferior temporal gyrus	33, 3, −42 (3.43)	
Fusiform gyrus	33, −6, −39 (4.51)	
Parietal		NO AREAS
Postcentral gyrus	−51, −9, 39 (4.88)	
	51, −12, 30 (4.91)	
Supramarginal gyrus	66, −21, 27 (3.97)	
Occipital		
Medial occipital cortex	36, −81, 3 (3.79)	
Inferior occipital cortex	39, −90, 0 (3.82)	
Subcortical		
Anterior cingulate cortex	3, 12, 27 (4.18)	
	Unpleasant pictures	
	Large LPP	Small LPP
	NO AREAS	NO AREAS

Table 4

Regions connected with amygdala for large LPP trials and small LPP trials

Anatomical Regions	MNI coordinates x,y,z (Z score)	
	Pleasant pictures	
	Large LPP	Small LPP
Dorsolateral prefrontal cortex	−27, 15, 51 (4.41)	NO AREAS
Temporal pole	27, 9, −27 (4.50)	
	Unpleasant pictures	
	Large LPP	Small LPP
Frontal		
Dorsolateral prefrontal cortex	−42, 51, 18 (3.79)	
	45, 12, 54 (4.02)	
Orbitofrontal cortex	3, 54, −3 (3.80)	39, 27, −21 (4.18)
Inferior frontal gyrus	48, 18, 0 (3.55)	
Supplementary motor area	−3, −9, 63 (3.32)	
Temporal		
Superior temporal gyrus	−54, 6, −6 (4.22)	−57, 6, −9 (3.85)
	54, −3, −9 (3.85)	60, 3, −12 (4.27)
Middle temporal gyrus	−51, −18, −15 (3.42)	−57, −18, −18 (4.44)
	54, −21, −15 (3.92)	57, −15, −15 (3.73)
Inferior temporal gyrus	54, −15, −21 (4.79)	51, −18, −21 (4.30)
	−63, −24, −21 (4.57)	−63, −24, −18 (3.98)
Temporal pole	45, 15, −21 (4.46)	54, 9, −18 (3.70)
	−57, 6, 0 (4.10)	−57, 9, −3 (3.51)
Fusiform gyrus	−24, −33, −18 (4.01)	−24, −33, −18 (4.15)
Fusiform gyrus	36, −27, −21 (3.86)	
Parietal		
Superior parietal cortex	−24, −48, 63 (4.86)	
Angular gyrus	42, −63, 51 (4.87)	42, −63, 45 (4.85)
Precuneus	−12, −45, 48 (3.21)	
	15, −42, 42 (4.10)	
Occipital		
Lingual gyrus	−24, −60, −3 (4.20)	−15, −51, −9 (4.31)
Lingual gyrus	18, −45, 9 (3.33)	
Calcarine	18, −66, 15 (4.95)	21, −69, 18 (3.90)
Subcortical		
Anterior cingulate cortex	3, 33, 15 (3.60)	0, 30, 15 (4.79)
Middle cingulate cortex	−3, −15, 39 (3.23)	0, −15, 42 (3.38)
Insula	−39, 15, −3 (3.75)	−42, 15, −3 (3.61)
Insula	36, 21, 6 (4.14)	
Parahippocampal gyrus/Hippocampus	−33, −3, −27 (4.16)	

Anatomical Regions	MNI coordinates x,y,z (Z score)	
	Pleasant pictures	
	Large LPP	Small LPP
Thalamus	21, −39, −9 (3.17) −6, −9, 0 (4.51)	